

Accepted Manuscript

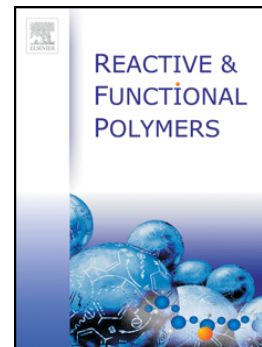
Self-assembled spin-labeled nanoparticles based on poly(amino acids)

A.V. Hubina, A.A. Pogodaev, V.V. Sharoyko, E.G. Vlach, T.B. Tennikova

PII: S1381-5148(16)30017-7
DOI: doi: [10.1016/j.reactfunctpolym.2016.01.018](https://doi.org/10.1016/j.reactfunctpolym.2016.01.018)
Reference: REACT 3626

To appear in:

Received date: 20 July 2015
Revised date: 22 January 2016
Accepted date: 28 January 2016



Please cite this article as: A.V. Hubina, A.A. Pogodaev, V.V. Sharoyko, E.G. Vlach, T.B. Tennikova, Self-assembled spin-labeled nanoparticles based on poly(amino acids), (2016), doi: [10.1016/j.reactfunctpolym.2016.01.018](https://doi.org/10.1016/j.reactfunctpolym.2016.01.018)

This is a PDF file of an unedited manuscript that has been accepted for publication. As a service to our customers we are providing this early version of the manuscript. The manuscript will undergo copyediting, typesetting, and review of the resulting proof before it is published in its final form. Please note that during the production process errors may be discovered which could affect the content, and all legal disclaimers that apply to the journal pertain.

Self-assembled spin-labeled nanoparticles based on poly(amino acids)A.V. Hubina^{a,b}, A.A. Pogodaev^a, V.V. Sharoyko^a, E.G. Vlakh^a and T.B. Tennikova^{a,*}

^a*Institute of Chemistry, Saint-Petersburg State University,
Universitiesky pr. 26, 198504 St. Petersburg, Russia*

^b*Institute of Macromolecular Chemistry, National Academy of Science of Ukraine,
Kharkivske shose 48, 02160, Kyiv, Ukraine*

*Corresponding author: Prof. Dr. Chem. Sci. Tatiana B. Tennikova

E-mail: tennikova@mail.ru

Tel. (++ 7 812) 323 1050

Fax: (++7 812) 328 6869

Abstract

The development of detectable nanoparticles for controlled drug delivery systems has tremendous practical importance regarding the monitoring of drug pathway in organism. Self-assembly amphiphilic block-copolymer poly(*L*-glutamic acid)-*b*-poly(*L*-phenylalanine) (pGlu-*b*-pPhe) was chosen for the preparation of discussed nanoparticles. The synthesis of blocks was carried out using ring-opening polymerization (ROP) of *N*-carboxyanhydrides of mentioned amino acids. To introduce the spin label at C-terminal position of hydrophilic block, (4-amino-2,2,6,6-tetramethylpiperidin-1-yl)oxyl (4-amino-TEMPO) was applied as ROP initiator and the polymerization of hydrophobic block was carried out with previously synthesized macroinitiator. The results obtained by transmission electron microscopy clearly showed that TEMPO-pGlu-*b*-pPhe polymer was really capable to self-assembling in aqueous solutions followed by polymersomes formation. The mean size of nanoparticles was increased in a range TEMPO-pGlu₄₃-*b*-pPhe₁₂ < TEMPO-pGlu₄₃-*b*-pPhe₂₉ < TEMPO-pGlu₄₃-*b*-pPhe₄₉ as 60 < 200 < 280 nm, respectively. EPR spectroscopy of the solutions of spin-labeled homopolymer TEMPO-p- γ -Glu(Bzl), block copolymers TEMPO-p- γ -Glu(Bzl)-*b*-pPhe and suspension of polymersomes formed from TEMPO-p-Glu-*b*-pPhe was performed and the results were compared. It was proved that in the case of nanoparticles EPR detectable spin labels are located on polymersome surface. The experiments in cell culture demonstrated the absence of cytotoxicity of labeled nanoparticles. Additionally, it was shown that TEMPO-label can be detected inside the cell by EPR method.

Keywords: poly(amino acids); spin label; polymersomes; ring-opening polymerization of *N*-carboxyanhydrides.

1. Introduction

In recent decades the preparation of nanoparticles for controlled drug delivery is on frontier of biomedical chemistry challenges. A wide variety of nanoparticles composed of lipids, natural and synthetic polymers, as well as inorganic materials have been developed [1]. To date, the known nanoparticulate drug delivery systems, depending on their nature and method of preparation, can have different design. For example, these particles can represent solid beads, nanospheres, nanocapsules, as well as self-assembled nanostructures of different morphology [1, 2].

Self-assembling has revolutionized soft materials research by enabling the efficient and high-throughput fabrication of ordered nanostructures for drug delivery [3]. For decades, self-assembled vesicles comprised low-molecular mass compounds such as phospholipids (liposomes) [4] or surfactants [5]. More recently, amphiphilic polymers have been shown to form very elaborated architectures and to serve as useful nanocontainers in aqueous solution [6, 7]. The self-assembly of amphiphilic block copolymers in appropriate media can form a variety of supramolecular assemblies including spherical, worm and multicompartiment micelles, as well as vesicles (or *polymersomes*). Polymersomes represent the liposome-like polymeric spheres with aqueous core surrounded by double layer polymer membrane. The aqueous core can be utilized for the encapsulation of hydrophilic therapeutics such as low-molecular mass substances, peptides, proteins (including enzymes), oligonucleotides and nucleic acids [8, 9]. In its turn, the hydrophobic part of membrane can integrate hydrophobic drugs [10].

Comparing to liposomes, polymersomes have thicker membrane resulting in less permeability for outside medium that, in turn, leads to their higher stability, storage capabilities [11, 12], as well as prolonged circulation time [13]. Moreover, block-copolymer chemistries can be tuned through polymer synthesis to yield polymersomes with diverse functionality [14, 15]. The composition and molecular weight of these polymersomes can be varied that leads to the formation of polymersomes not only with different chemical nature, size and responsiveness to stimuli but also different membrane thickness and permeability [16].

A lot of synthetic polymers are discussed in the literature regarding to their ability to serve as building blocks for polymersomes [17, 18]. Nevertheless, poly(amino acids) and polypeptides can be related to one of the most promising types of macromolecules. These bio-inspired polymers possess biodegradability and biocompatibility that, in particular, are the main features for construction of modern drug delivery systems. Besides, further modification of polymersomes is possible due to functional groups on the surface [19-21].

Drug delivery and release is a complex process, which demands powerful modern tools for tracking in time drug delivery carrier's diffusion and stability. Electron Paramagnetic Resonance (EPR) spectroscopy represents direct, sensitive and non-invasive method, which can be applied both *in vitro* and *in vivo*. Furthermore, electron paramagnetic resonance imaging allows visualizing traces and spatial distribution of drug carriers [22, 23]. The EPR spectroscopy concerns investigation of the compounds that contain paramagnetic centers. In the case if the polymer does not have such centers, the spin-labeling approach can be used. Stable nitroxide radicals of various structure and functionality are widely used as spin probes or spin labels for biochemical applications, including investigation of biopolymers (proteins) [22-26]. They demonstrate stability at physiological temperature and pH, and the versatility of functional groups, which they can contain. It opens a lot of pathways to attach the paramagnetic label to the polymer.

In current literature (2,2,6,6-tetramethylpiperidin-1-yl)oxyl (TEMPO) and its derivatives are mostly mentioned as spin probe/spin label or capping agents and mediators in free radical polymerization and oxidative processes [27, 28, 29]. In [30] the method of fabrication of EPR detectable amphiphilic block copolymers was proposed. The spin label, namely, 4-amino-TEMPO was attached to the hydrophilic block of synthesized poly(*N*-isopropyl methacrylamide-co-*N*-isopropyl maleamic acid-co-10-undecenoic acid). The pH- and thermo-sensitive micelles were assembled in aqueous solution, and the EPR was applied to control the process of micelle formation and destruction under various pH and temperature conditions. Polymer-coated TEMPO-labeled inorganic nanoparticles were also synthesized and investigated [31]. The possibility

of EPR-imaging of spatial distribution of nanoparticles obtained was shown using EPR in L-band region. However, there is no reference in the literature to application of spin label as initiator of ring-opening polymerization (ROP) of *N*-carboxyanhydrides of amino acids.

In this paper the formation of polymer nanoparticles from amphiphilic copolymers based on poly(*L*-glutamic acid)-*b*-poly(*L*-phenylalanine) (pGlu-*b*-pPhe) with covalently attached 4-amino-TEMPO spin label is discussed. The mentioned label was used as initiator for ROP of α -*N*-carboxyanhydride of γ -benzyl-*L*-glutamate. This approach allowed the introduction of spin label into C-terminal position of synthesized poly(amino acid). The labeled macroinitiator was further used for copolymerization of hydrophobic pPhe block. Finally, after amphiphilic copolymer self-assembly the label appeared to be located on the outer (hydrophilic) nanoparticle surface that is very important for sensitive ESR-imaging.

2. Experimental section

2.1. Materials

γ -benzyl-*L*-glutamate, *L*-phenylalanine, triphosgene, α -pinene, 4-amino-TEMPO, (3-aminopropyl)triethoxysilane (APTES), trifluoromethanesulfonic acid (TFMSA), trifluoroacetic acid (TFA) and other reagents were purchased from Sigma–Aldrich (Germany) and used as received. 1,4-Dioxan, *n*-hexan, *N,N*-dimethylformamide (DMF), ethyl acetate and other solvents were purchased from Acros (Russia) and distilled before application.

2.2. Methods

2.2.1. Synthesis of *N*-carboxyanhydrides (NCAs)

NCAs of γ -Glu-(Bzl) and Phe were synthesized using routine procedure reported, in particular, in [32]. Dioxane was used as a solvent, and both acquired NCA were purified by recrystallization from ethyl acetate/*n*-hexane. Yields: NCA of γ -Glu-(Bzl) – 75%, NCA of Phe – 70%. Structure and purity level of synthesized NCAs were confirmed by ^1H NMR. Spectra were

recorded at room temperature (298 K) using Bruker 400 MHz Avance instrument (Germany) and the samples dissolved in CDCl_3 . $^1\text{H-NMR}$: NCA of γ -Glu-(Bzl) – 2.05 – 2.39 (m, 2 H), 2.63 (t, 2 H), 4.39 (t, 1 H), 5.17 (s, 2 H), 6.40 (br. s., 1 H), 7.39 (m, 5 H), NCA of Phe – 2.94–3.35 (m, 2H), 4.55 (m, 1H), 5.60 (s, 1H), 7.19–7.41 (m, 5H).

2.2.2. Polymerization

The homopolymer of γ -Glu(Bzl) was synthesized via NCA polymerization in dry dioxane using 4-amino-TEMPO as initiator. The monomer/initiator molar ratio was equal to 25. After reaction for 24 hours at 30°C , the product was precipitated in excess of diethyl ether and dried. Precipitation procedure from dioxane/diethyl ether was performed twice. The yield of the homopolymer was 67%. The APTES initiated polymerization of γ -Glu(Bzl) NCA was carried out in the same way with the yield of the homopolymer product equal to 75%.

Both prepared TEMPO- p - γ -Glu(Bzl) and APTES- p - γ -Glu(Bzl) were used as macroinitiator for Phe-NCA polymerization. For that, three polymerization mixtures differed with molar monomer/initiator ratios (100, 150 and 200), featuring TEMPO- p - γ -Glu(Bzl) as macroinitiator were prepared in anhydrous and amine free DMF and incubated at 30°C for 24 hours. Then reaction product was isolated by precipitation in diethyl ether, purified twice using DMF/diethyl ether mixture. Finally, p - γ -Glu(Bzl)- b - p Phe was collected after centrifugation and dried. The same procedure was carried out for APTES- p - γ -Glu(Bzl)/Phe-NCA taken as 1:100.

2.2.3. Polymer characterization

The gel permeation chromatography (GPC) measurements were performed on a Shimadzu LC-20 Prominence system with refractometric RID 10-A detector (Japan) using 7.8×300 mm Styragel Column, HMW 6E, 15-20 μm bead size (Waters, USA). The analysis was carried out at 60°C using DMF with 0.1 M LiBr as eluent. The mobile phase flow rate was 0.3 mL/min. Molecular weights and molecular weight distributions for γ -Glu(Bzl) homopolymer were calculated

using poly(methyl methacrylate) standards in M_w range from 17,000 to 250,000 with polydispersity lower than 1.14. The calculations were carried out with GPC LC Solutions software (Shimadzu, Japan).

The contribution of hydrophobic block was evaluated using chromatographic amino acid analysis after total hydrolysis of polymer samples. The hydrolysis of 1 mg of a sample was carried out in 2 mL of 6 M HCl with 0.0001% phenol in vacuum-sealed ampoule during 4 days. The solvent was evaporated several times with water to eliminate HCl and finally to reach neutral pH. The products of hydrolysis were analyzed by reversed phase (RP) HPLC using LCMS-8030 Shimadzu system with triple quadruple mass-spectrometry detection (LC-MS) (all from Shimadzu, Japan), equipped with 2x150 mm Luna C₁₈ column, packed with 5 μ m particles. The isocratic elution mode was applied and 0.1% acetonitrile/HCOOH in ratio 5/95 wt% was used as eluent. The mobile phase flow rate was equal to 0.3 mL/min.

2.2.4. Preparation of polymersomes

The Bzl-protection group of p- γ -Glu(Bzl)-*b*-pPhe was removed by TFMSA/TFA mixture in ratio 1:10 at 22°C. Then the product was dispersed in DMSO, put into dialysis membrane bag MWCO 1000 and dialyzed against 0.1 M Na-borate buffer solution, pH 8.6, for 1 day. After 2 days of freeze drying, pGlu-*b*-pPhe was collected.

Polymer nanoparticles were prepared by dispersing the copolymer in 0.1 M Na-borate buffer solution, pH 8.6, at a concentration of 0.5 and 0.25 mg/mL. The dispersion was sonicated at 30°C for 2 hours.

2.2.5. Dynamic Light Scattering (DLS)

DLS measurements were performed on Laser Particle Analyzer SZ100 (Horiba Jobin Yvon, Japan) at scattering angle 90° at 25°C. The range of concentrations of nanoparticles in Na-borate buffer solution, pH 8.7, was 1.0, 0.5 and 0.25 mg/mL.

2.2.6. Transmission electron microscopy (TEM)

The nanoparticles obtained were analyzed using a transmission electron microscope (Jeol JEM-2100, Japan) operated at an acceleration voltage of 160 kV, after negatively staining the solution with 2% (w/v) uranyl acetate.

2.2.7. EPR spectroscopy

The homopolymer, block-copolymer and deprotected block-copolymer were investigated by EPR spectroscopy. The spin probe TEMPO was non-covalently incorporated into APTES-p- γ -Glu(Bzl), APTES-p- γ -Glu(Bzl)-*b*-pPhe and APTES-pGlu-*b*-pPhe in vapors at 50°C as it was described in [33]. Nanoparticle suspensions were prepared in concentration 0.5 mg/mL. EPR spectra were recorded at 25°C using Bruker Elexsys 580 spectrometer (X-band) (Germany) with high sensitivity resonator. General instrument settings were as follows:

Solid samples with spin probe: microwave power 150 mW, microwave frequency 9.87 GHz, modulation frequency 100 kHz, modulation amplitude 1.0 G, sweep width 100 G, central field value 3370 G, sweep time 200 s. Measurements were performed using 50 μ L capillary tubes.

Nanoparticle suspension: microwave power 751.8 mW, microwave frequency 9.77 GHz, modulation frequency 100 kHz, modulation amplitude 1.5 G, sweep width 75 G, central field value 3482.5 G; sweep time 20.40 s. Measurements were performed using 500 μ L tube for liquid samples.

The rotation correlation time was calculated using the equation:

$$\tau = 6.65 \cdot \Delta H_+ \left(\sqrt{\frac{I_-}{I_+}} - 1 \right) \cdot 10^{-10} \quad (1)$$

where ΔH_+ is line width of high-field component, I_+ - line height of high-field component I_- - line height of low-field component.

For the calculation of the anisotropy parameter ε , the following equation was used:

$$\varepsilon = \frac{\sqrt{\frac{I_0}{I_+}} - 1}{\sqrt{\frac{I_0}{I_-}} - 1} \quad (2)$$

where I_0 , I_+ and I_- are line heights of central, high-field and low-field component, respectively.

To evaluate the size of nanoparticles, Stokes-Einstein equation was applied:

$$\tau = \frac{4\pi\eta R^3}{3kT} \quad (3)$$

where η is solvent viscosity, R is effective hydrodynamic radius of the molecule, k is Boltzmann constant and T is temperature.

The EPR experiment with nanoparticle/cell suspension was carried out under the following EPR spectrometer tunings: microwave power 751.8 mW, microwave frequency 9.77 GHz, modulation frequency 100 kHz, modulation amplitude 1.5 G, sweep width 100 G, central field value 3482 G; sweep time 25 s. The measurements were performed using 500 μ L tube for liquid samples.

Incubation mixtures consisted of U937 cells resuspended to 1×10^6 cells/ml in RPMI 1640 medium in new disposable tubes. The suspension of TEMPO-pGlu₄₃-b-pPhe₂₉ (final concentration is 0.5 mg/mL) was added to cell suspension. The contents of the tube were gently mixed by vortexing, then transferred to an EPR flat cell and incubated at 37°C during 1 hour. EPR spectra were recorded each 40 minutes within 24 hours.

2.2.8. Cytotoxicity assay

Cells were routinely cultured at 37°C in humidified atmosphere containing air and 5% CO₂. Human embryonic kidney cells (HEK 293), human epithelial colorectal adenocarcinoma cells (Caco-2) and human lung lymphoblasts (U937) were obtained from BioloT (Saint Petersburg, Russian Federation) and were grown in Dulbeccos Modified Eagle's Medium (BioloT) containing 10% (v/v) heat-inactivated fetal bovine serum (FBS, HyClone Laboratories, UT,

USA), 1% L-glutamine, 1% sodium pyruvate, 50 U/mL penicillin, and 50 µg/mL streptomycin (BioloT).

Toxicity of polymer nanoparticles was assessed using a standard colorimetric assay with tetrazolium dye – 3-(4,5-dimethylthiazol-2-yl)-2,5-diphenyltetrazolium bromide (MTT). The cells were incubated for 48 h with fresh medium containing different concentrations of polymer nanoparticles. Following treatment, Dulbeccos Modified Eagle's Medium (100 µL/ well) and 20 µL of a 2.5 mg/mL MTT solution were added and cells were incubated for 1 h at 37 °C. The used cell density was 10×10^3 cells/200 µL/well in 96-well microtiter plates. After careful removal of the supernatants, the MTT-formazan crystals formed by metabolically viable cells were dissolved in DMSO (100 µL/well) and absorbance was measured at 540 nm and 690 nm in a multiwell plate reader. Values measured at 540 nm were subtracted for background correction at 690 nm, and the data were plotted as a percent of control samples using Microsoft Excel.

2.2.9. Dye encapsulation and cell imaging

To investigate the cellular uptake the TEMPO-pGlu₄₃-b-pPhe₂₉ sample was stained with the photosensitizer Fotoditazin[®]. For this, 0.2 mL of dye was dissolved in 0.8 mL of distilled water. 2.0 mg of TEMPO-pGlu₄₃-b-pPhe₂₉ suspended in 1.0 mL of 0.1 M PBS solution, pH 7.4, was mixed with 1.0 mL dye solution and sonicated for 2 h. Excess of dye was removed via dialysis through membrane (12 kDa MWCO).

Then, the stained sample was added to the U937 cells suspension (1×10^6 cells/ml) in RPMI 1640 medium to obtain the final concentration of polymersomes 0.5 mg/mL. The sample obtained was incubated during 1 hour and then the images were taken using multiphotonic confocal scanning microscope Leica TCS SP5 MP at 662 nm.

3. Results and discussion

3.1. Synthesis and investigation of spin labeled poly(amino acids)

The localization of the spin label in block copolymers is of the great importance because it brings information about the way the self-assembly was performed [26]. The terminal residence of spin label attached to the end of the hydrophilic block of the self-assembling block copolymer opens the possibility to obtain detectable nanoparticles with the label located directly on the surface of the polymeric vesicle. Following this idea, 4-amino-TEMPO was applied as initiator for the NCA polymerization of γ -Glu(Bzl) (**Scheme 1**). The TEMPO-*p*- γ -Glu(Bzl) with molecular weight 10225 (43 amino acid residues) and narrow molecular weight distribution ($M_w/M_n = 1.1$) was synthesized. At second step the TEMPO-*p*- γ -Glu(Bzl) was used as macroinitiator for NCA polymerization of Phe. The synthesized samples were insoluble in organic solvents and the characterization of hydrophobic block length of co-polymers by GPC or in solution NMR was impossible. Thus, to evaluate the hydrophobic block length, the resulting copolymers were totally hydrolyzed as it was described in 2.2.3. Then the hydrolyzed samples were investigated by RP HPLC (see Supplementary, Figure S1). Afterwards, using L-glutamic acid and L-phenylalanine concentration obtained in each sample (see Supplementary, Table S1) along with the GPC data of TEMPO-*p*- γ -Glu(Bzl), the contribution of hydrophobic block was evaluated. Particularly, three samples of block copolymer with different length of hydrophobic block, namely, TEMPO-*p*- γ -Glu(OBzl)₄₃-*b*-pPhe₄₉, TEMPO-*p*- γ -Glu(OBzl)₄₃-*b*-pPhe₂₉ and TEMPO-*p*- γ -Glu(OBzl)₄₃-*b*-pPhe₁₂ were obtained. The formation of amphiphilic block copolymers was achieved after deprotection of Bzl-protective group (**Scheme 1**).

To compare the results on magnetic properties of copolymers containing terminal spin label (4-amino-TEMPO) strictly located in hydrophilic part of the block copolymer to those bearing non-covalently incorporated paramagnetic molecule (spin probe TEMPO), the samples of diamagnetic *p*- γ -Glu(OBzl)-*b*-pPhe for spin probe incorporation was synthesized using APTES as initiator. The APTES- *p*- γ -Glu(OBzl) molecular mass characteristics were the following: $M_n=13800$ (62 amino acid residues) and molecular weight distribution $M_w/M_n = 1.2$. The final block copolymer was of the following structure APTES-*p*- γ -Glu₆₂-*b*-pPhe₂₉.

The EPR spectra were recorded for all the intermediate and resulting polymer compounds: TEMPO- p - γ -Glu(BzL), TEMPO- p - γ -Glu(BzL)- b -pPhe and deprotected TEMPO- p Glu- b -pPhe in solid, as well as for the same series of model APTES-initiated analogue block copolymers (APTES- p - γ -Glu(BzL), APTES- p - γ -Glu(BzL)- b -pPhe and APTES- p Glu- b -pPhe) with spin-probe incorporated into polymers in vapors.

The line shape, symmetry, and width of the EPR spectra for spin probe non-covalently introduced into APTES-initiated polymer matrices differ sufficiently from the spectra of the spin-labeled polymer samples obtained at polymerization step (**Figure 1**). The parameters of $2A_{\parallel}$ and g were calculated and given in **Table 1**.

First, the data for spin probe samples were analyzed. The spectra of TEMPO in APTES- p - γ -Glu(BzL), APTES- p - γ -Glu(BzL)- b -pPhe and APTES- p Glu- b -pPhe are the triplets with asymmetric widened components (**Figure 1a**). The line shape of the all spectra revealed the anisotropy of the constant of hyperfine coupling. All the spectra have split high-field and low-field components that is the evidence of the existing at least two different populations of paramagnetic particles [34]. It may be caused by the localization of the TEMPO in the domains with different molecular dynamics. For APTES- p - γ -Glu(BzL) and APTES- p Glu(BzL)- b -pPhe the contribution of one type ($A_{\parallel 1}$) prevails against another ($A_{\parallel 2}$) while for APTES- p Glu- b -pPhe no noticeable dominance of any of the types was observed. Thus, the character of the spin probe behavior is similar both in hydrophobic protected polymer matrix and in block copolymer containing two hydrophobic blocks. After deprotection the remarkable difference between two populations of nitroxide radical is, mainly, explained by the presence of hydrophilic and hydrophobic blocks in APTES- p Glu- b -pPhe. Still the g -factor is also changed from APTES- p - γ -Glu(BzL) to APTES- p Glu- b -pPhe.

The spectrum of poly(γ -benzyl ester of glutamic acid) synthesized *via* ROP with 4-amino-TEMPO has broad line shape. In contrary to the free radical spectrum has poorly realized high-field component (**Figure 1b**). A number of publications [35; 36] confirms that such kind of

spectrum line shape is common for a spin-label covalently attached to macromolecular chain, which results into highly hindered rotation of the spin label due to the fixed position of the label.

Considering that 4-amino-TEMPO initiates ROP of γ -Glu(Bzl) NCA as primary amine, the amine mechanism of ROP is realized and the initiator is located at the C-terminal position of the poly(amino acid) chain [33]. The line shape and spectra parameters such as g-factor and A_{\parallel} did not changed after co-polymerization and further deprotection (**Table 1**). Besides, according to [35 - 37] the line shape of the EPR spectrum of the spin-labeled protein is in dependence on position of the spin label in the molecule. Considering on the constant spectra parameters for all spin-labeled samples, it is obvious that EPR detectable fragment preserves the location in the end of the hydrophilic chain of the final amphiphilic block copolymer, and no radicals are distributed in other domains of the polymer matrix.

3.2. Morphology and size distribution of self-assembled nanoparticles

The morphology of the prepared nanoparticles was investigated by TEM. As it can be seen on the **Figure 2**, the formed particles can be identified as polymer vesicles with double-layered membrane. Considering that the hydrophobic block is presented by poly(phenylalanine), the observed structure can be formed due to π - π interactions between aromatic fragments of hydrophobic chains. Though the particle size differs with the growth of hydrophobic part of the macromolecule, the morphology for all samples remains the same. According to the published data, the liposome-like nanoparticles (polymerosomes) can be prepared with the hydrophilic part contribution under 45% [38], but for the nanoparticles obtained in present research the polymerosomes were assembled even at the dominance of hydrophilic block part.

As it can be seen from DLS data (**Figure 3**), the hydrodynamic diameter of prepared nanoparticles inversely depended on the length of the hydrophobic block. The mean nanoparticle size increased in the row $\text{pGlu}_{43}\text{-}b\text{-pPhe}_{12} < \text{pGlu}_{43}\text{-}b\text{-pPhe}_{29} < \text{pGlu}_{43}\text{-}b\text{-pPhe}_{49}$ as $60 < 200 < 280$ nm, respectively. According to ζ -potential values that were about -20 mV at pH 8.6 at poly-

mer concentration 0.5 mg/mL, all samples formed stable nanoparticles with negative surface charge.

All samples exhibited evident dependence of particle size distribution on polymer concentration. Thus, with the concentration growth from 0.25 mg/mL to 1.00 mg/mL the mean size of nanoparticles increased.

3.3. EPR investigation of self-assembled nanoparticles

After the self-assembly was performed in sodium borate buffer, pH 8.6, at polymer concentration of 0.5 mg/mL, the EPR spectra of suspensions obtained were recorded. Comparing to the solid samples, the EPR spectra of all samples changed sufficiently comparing to the solid sample spectra (**Figure 4**). The spectra of suspensions are isotropic and symmetric with three well-defined components and are similar to the line shape of the spectrum of free 4-amino-TEMPO radical diluted in the same buffer solution (**Figure 4**). The values of τ were high (**Table 2**). Such line shape and line width prove the absence of spin-spin interactions between neighboring spin-labels both in the membrane of one nanoparticle and between 4-amino-TEMPO residues from different nanoparticles. All spectra are characterized with similar value of hyperfine coupling constant $a_N \approx 17.9$ G. It is known from the literature that the value of hyperfine coupling constant is the characteristic of medium polarity [26]. The values calculated for all samples confirm that the spin labeled end of polymer chain is located on the surface of the nanoparticle in polar medium (**Figure 4**). Considering that only spin-labels located on the surface are EPR-responsive, the amount of the responsive centers can be valued from EPR data *via* calculating the integral intensity of the each sample spectrum and comparing it to the standard solutions of the 4-amino-TEMPO. The concentration of spin labels in nanoparticle suspension was calculated using the linear approximation of integral intensity dependence on the concentration of 4-amino-TEMPO solutions.

The integral intensity of the EPR spectrum of nanoparticle suspensions increased in the raw pGlu₄₃-*b*-pPhe₂₉ to pGlu₄₃-*b*-pPhe₄₉. This result corresponds to the change of nanoparticle hydrodynamic diameter (DLS data), revealing that the growth of nanoparticle diameter leads to increasing of the concentration spin labels on the surface.

The possibility of nanoparticle hydrodynamic diameter determination *via* EPR data was discussed in the work [26]. Particularly, the correlation rotation time value calculated from EPR spectrum can be applied in Stokes-Einstein equation to evaluate the nanoparticle size (see Experimental part). This method is efficient in the case if only the motion of the whole nanoparticle is considered, while the self-rotation of the spin probe against the nanoparticle is neglected. Using this assumption, the hydrodynamic radiuses of the samples were calculated (**Table 2**). The results were opposite to the TEM and DLS data obtained. It means that τ values obtained from EPR data cannot characterize the motion and the size parameters of the nanoparticles.

Then the approach of determination of the segmental mobility discussed in [40] was applied. According to the above-mentioned work, the covalently attached spin label simultaneously takes part in two types of motion: oscillation near the segment and in slow isotropic motion with the segment of the macromolecule. Considering on the dependence of rotation correlation time on viscosity of the solvent, the Stokes-Einstein equation (3) can be applied to determine the effective radius of the segment. Thus, the insufficient changes of τ values can be explained by different size of spin labeled macrochain fragment and its distance from the hydrophobic part of the membrane due to the dependence of the membrane thickness on the hydrophilic/hydrophobic block balance.

3.4. Cell experiments

It was a principal part of the research to investigate if the TEMPO-bearing nanoparticles can be detected inside the cells *via* EPR method.

First of all, the TEMPO-bearing nanoparticles obtained were tested regarding to their cytotoxicity using standard MTT assay and three cell lines. Suspensions of TEMPO-pGlu₄₃-b-pPhe_x nanoparticles at four different concentrations ranging from 0.125 to 2.00 mg/mL were incubated with cells within 48 h. As can be seen from **Figure 5** illustrating the data for pGlu₄₃-b-pPhe₄₉ the cell viability was higher than 85% for all tested concentrations that means the absence of cytotoxicity during the studied time period.

To detect if the nanoparticles penetrate into the cells, the TEMPO-pGlu₄₃-b-pPhe₂₉ polymersomes containing encapsulated fluorescent dye Fotoditazin were incubated with the U937 cells and then investigated by confocal microscopy. The coloration of inner space of cells by encapsulated dye proved the cellular uptake of nanoparticles developed (**Figure 6**).

Figure 7 presents the EPR spectrum of TEMPO-pGlu₄₃-b-pPhe₂₉ after its penetration into U937 cells. The spectrum has the line shape similar to the spectrum of the respective initial nanoparticle suspension (**Figure 4**). The hyperfine coupling constant value a_N is also about 17.5 G, which is similar to the nanoparticle suspensions. The calculated value of rotation correlation time (τ) is 5.02×10^{-10} s that does not differ from the value of τ of the nanoparticle suspension. Thus, the approach suggested can be applied as an effective imaging tool in biomedicine, particularly, for monitoring of new drug system distribution in tissues at bioapprobation step.

4. Conclusions

A new approach of synthesis of spin labeled poly(amino acid)-based nanoparticles was developed. The series of amphiphilic block copolymers with different hydrophobic part length was synthesized using the spin label 4-amino TEMPO as initiator of NCA ROP at the first stage of synthesis. The spin label was strictly located in the C-terminal position of hydrophilic poly(amino acid) chain of the resulting block copolymer.

The synthesized pGlu-*b*-pPhe samples were able to self-assembling in aqueous solutions forming polymersomes. The diameter of prepared nanoparticles depended on the length of hy-

drophobic block and polymer concentration. The increasing of the hydrophobic block contribution into polymer molecular weight led to the growth of nanoparticle size.

In suspension spin labels are located on polymersome surface and make them EPR detectable. The nanoparticle size defines the amount of the spin labels and depends on the hydrophobic/hydrophilic blocks balance. The rotation correlation time calculated from EPR data for all samples were the values of one order of magnitude and insignificantly grew in the row pGlu₄₃-*b*-pPhe₄₉<pGlu₄₃-*b*-pPhe₂₉<pGlu₄₃-*b*-pPhe₁₂ showing the dependence of TEMPO containing fragment size on the contribution of increasing hydrophobic block.

The spin-labeled nanoparticles were found to be biocompatible and successfully detected by EPR after penetrating the cell membrane. Thus, it makes possible to use the developed polymersomes for bioimaging purposes.

Acknowledgements

This work was supported by grant of Russian Scientific Foundation (# 14-50-00069). The participation in this work of Dr. A.V. Hubina (monthly salary) was supported by postdoc program from St. Petersburg State University (# 12.50.1193.2014).

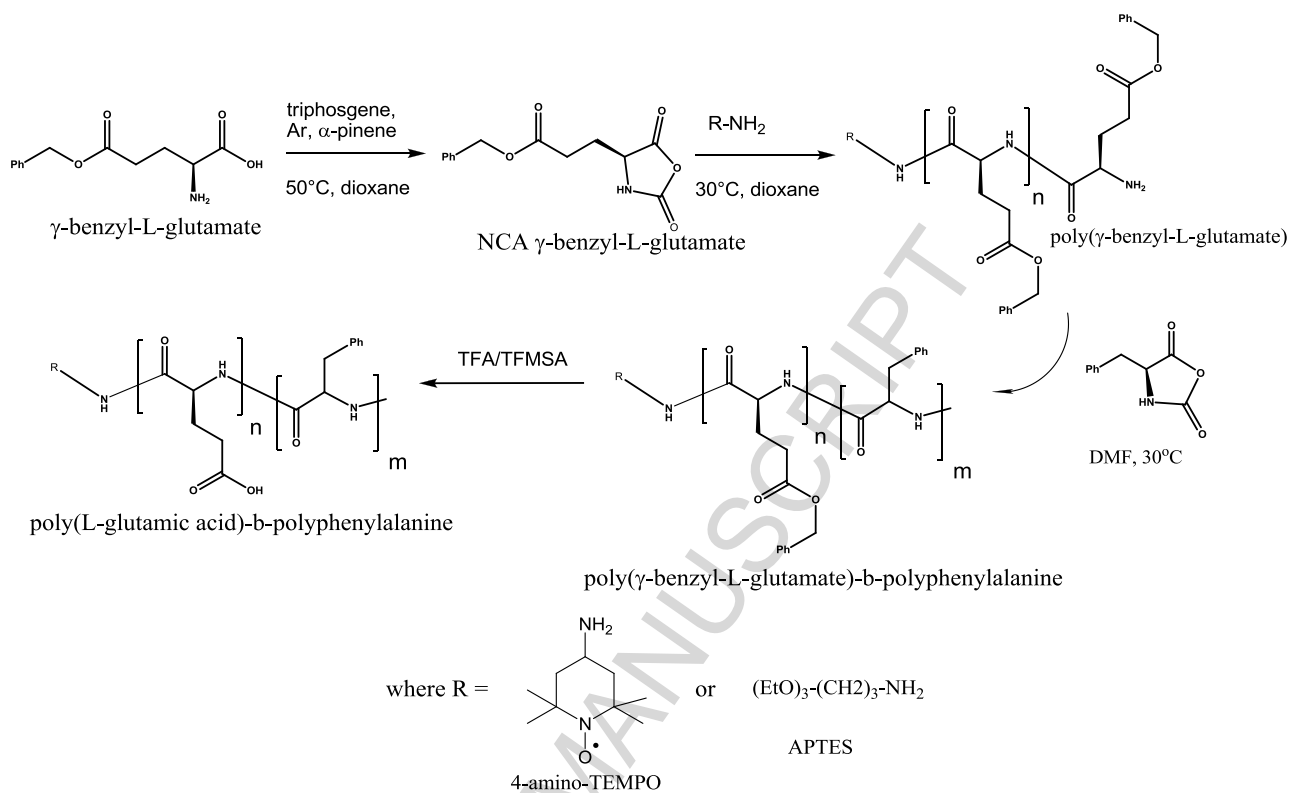
GPC and LC-MS were carried out in Chemical Analysis and Materials Research Centre. NMR and EPR experiments were performed in St. Petersburg State University Resource Center for Magnetic Resonance. The authors are very grateful to Dr. S.M. Sukharzhevskii for EPR measurements and result discussion. Cell experiments were carried out using the equipment of the Research Center on Development of Molecular and Cell Technologies of St. Petersburg State University.

References

- [1] A.Z. Wilczewska, K. Niemirowicz, K.H. Markiewicz, H. Car, *Pharmacol. Rep.* **2012**, *64*, 1020 – 1037.
- [2] K. Letchford, H. Burt, *European J. Pharmaceutics Biopharmaceutics*, **2007**, *65*, 259 - 269.
- [3] S. I. Stupp, V. Le Bonheur, K. Walker, L. S. Li, K. Huggins, M. Keser, A. Ams-tutz, *Science*, **1997**, *276*, 384 - 389.
- [4] G. Gregoriadis, B.E. Ryman, *Biochem. J.*, **1971**, *124*, 58 p.
- [5] A.D. Dinsmore, M.F. Hsu, M.G.Nikolaides, M.Marquez, A.R. Bausch, D.A. Weitz, *Science*, **2002**, *298*, 1006 - 1009.
- [6] S.E. Dunn, A. Brindley, S.S. Davis, M.C. Davies, L. Illum, *Pharm.Res.*, **1994**, *11*, 1016 - 1022.
- [7] K. Kita-Tokarczyk, J. Grumelard, T. Haefele, W. Meier, *Polymer*, **2005**, *46*, 3540 - 3563.
- [8] T.O. Pangburn, M.A. Petersen, B.Waybrant, M.M. Adil, E. Kokkoli, *J.Biomech. Eng. Trans. ASME*, **2009**, *131*, 120.
- [9] R. Brinkhuis, F.P.J.T. Rutjes, J.C.M. Hest, *Polym. Chem.*, **2011**, *2*, 1449 - 1462.
- [10] F. Ahmed, R.I. Pakunlu, A. Brannan, F. Bates, T. Minko, D.E. Discher, *J. Control Re-lease*, **2006**, *116*, 150 - 158.
- [11] J.C.M. Lee, H. Bermudez, B.M. Discher, M.A. Sheehan, Y.Y. Won, F.S. Bates, D.E. Discher, *Biotechnol. Bioengineer*, **2001**, *73*, 135 - 145.
- [12] F. Meng, G.H.M. Engbers, J. Feijen, *J. Control. Release*, **2005**, *101*, 187 - 198.
- [13] P.J. Photos, L. Bacakova, B. Discher, F.S. Bates, D.E. Discher, *J. Control. Release*, **2003**, *90*, 323 - 334.
- [14] J.S. Lee, J. Feijen, *J. Control. Release*, **2012**, *161*, 473 - 483.
- [15] N. Hadjichristidis, M. Pitsikalis, H. Iatrou, *Adv. Polym. Sci.*, **2005**, *189*, 1 - 124.
- [16] G. Battaglia, A.J. Ryan, S. Tomas, *Langmuir*, **2006**, *22*, 4910 - 4913.

- [17] J.S. Lee, J. Feijen, *J. Control. Release*, **2012**, *161*, 473 - 483.
- [18] K. Letchford, H. Burt, *Europ. J. Pharm. Biopharm.*, **2007**, *65*, 259 - 269.
- [19] A. Carlsen, S. Lecommandoux. *Current Opinion in Colloid&Interface Science*, **2009**, *14*, 329.
- [20] L. Zhao, N. Li, K. Wang, C. Shi, L. Zhang, Y. Luan. *Biomaterials*, **2014**, *35*, 1284.
- [21] C. Deng, J. Wu, R. Cheng, F. Meng, H.A. Klok, Z. Zhong. *Progress in Polymer Science*, **2014**, *39*, 330.
- [22] U. Eichhoff, P. Höfer. *Low Temp. Physics*, **2015**, *41*, 62 – 66.
- [23] S. Kempe, H. Metz, K. Mäder. *Eu. Jour. of Pharm. and Biopharm.*, **2010**, *74*, 55.
- [24] W.K. Subczynski, J. Widomska, J.B. Feix, *Free Radical Biology&Medicine*, **2009**, *46*, 707 - 718.
- [25] A.M. Wasserman, V.A. Kasaikin , V.P. Timofeev. *Spectrochimica Acta Part A*, **1998**, *54*, 2295.
- [26] A. M. Wasserman, *Rus. Chem. Rev.*, **1994**, *63 (5)*, 373 - 401.
- [27] A. Kaim, K. Pietrasik, T. Stoklosa, *Eu.Polym.Jour.*, **2010**, *46*, 519 - 527.
- [28] W. A. Braunecker, K. Matyjaszewski, *Progress in Polymer Science*, **2007**, *32*, 93 - 146.
- [29] A.M. Wasserman, L.L. Yasina, M.V. Motyakin, I.I. Aliev, N.A. Churochkina, L.Z. Rogovina. *Spectrochimica Acta Part A*, **2008**, *69*, 1344.
- [30] R. Yu, H. Zhao, Z. Zhao, Y. Wan, H. Yuan, M. Lan, L.F. Lindoy, G. Wei. *Journal of Colloid and Interface science*, **2011**, *362*, 584.
- [31] R. Krzyminiewski, T. Kubiak, B. Dobosz, G. Schroeder, J. Kurczewska, *Current Applied Physics*, **2014**, *14*, 798 - 804.
- [32] H. Leuchs. *Berichte der Deutschen Chemischen Gesellschaft*, **1906**, *39*, 857.
- [33] A. Wolinska-Grabczyk, W. Bednarski, A. Jankowski, S. Waplak. *Polymer*, **2005**, *46*, 2461.
- [34] A.N. Kuznetsov, *Spin Probe Method*, Nauka, Moscow, **1976**, p. 210 (in Russian).

- [35] M.P. Filatova, Z. Reissmann, T.O. Reutova, V.T. Ivanov, G.L. Grigoryan, A.M. Shapiro, E.G. Rozantsev. *Bioorganic Chemistry (in Russian)*, **1977**, 3, 1181 - 1189.
- [36] J. Pilar, D. Horak, J. Labsky, F. Svec, *Polymer*, **1988**, 29, 500 - 506.
- [37] J. Widomska, M. Raguz, J. Dillon, E.R. Gaillard, W.K. Subczynski, *Biochimica et Biophysica Acta*, **2007**, 1768, 1454 - 1465.
- [38] C. LoPresti, H. Lomas, M. Massignani, T. Smart, G. Battaglia. *Journal of Materials Chemistry*, **2009**. 19, 3557 - 3590.
- [39] A. Blanz, S. P. Armes, A. J. Ryan. *Macromol. Rapid. Commun.*, **2009**, 30, 267 – 277.
- [40] A.M. Wasserman, V.A. Kasatkin, V.P. Timofeev, *Spectrochimica Acta Part A*, **1998**, 54, 2295 - 2308.



Scheme 1. Synthesis of TEMPO-pGlu-b-pPhe block copolymers.

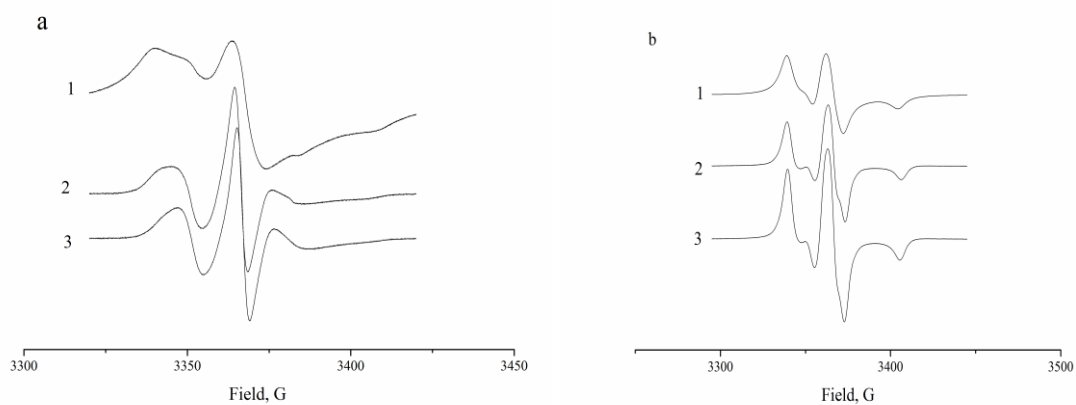


Figure 1. EPR spectra of non-covalently introduced spin-probe (A) 1 - APTES-p-γ-Glu(Bzl), 2 - APTES-p-γ-Glu(Bzl)-b-pPhe, 3 - APTES-pGlu-b-pPhe; and covalently attached spin label (B) 1- TEMPO-p-γ-Glu(Bzl), 2 - TEMPO-p-γ-Glu(Bzl)-b-pPhe, 3 - TEMPO-pGlu-b-pPhe.

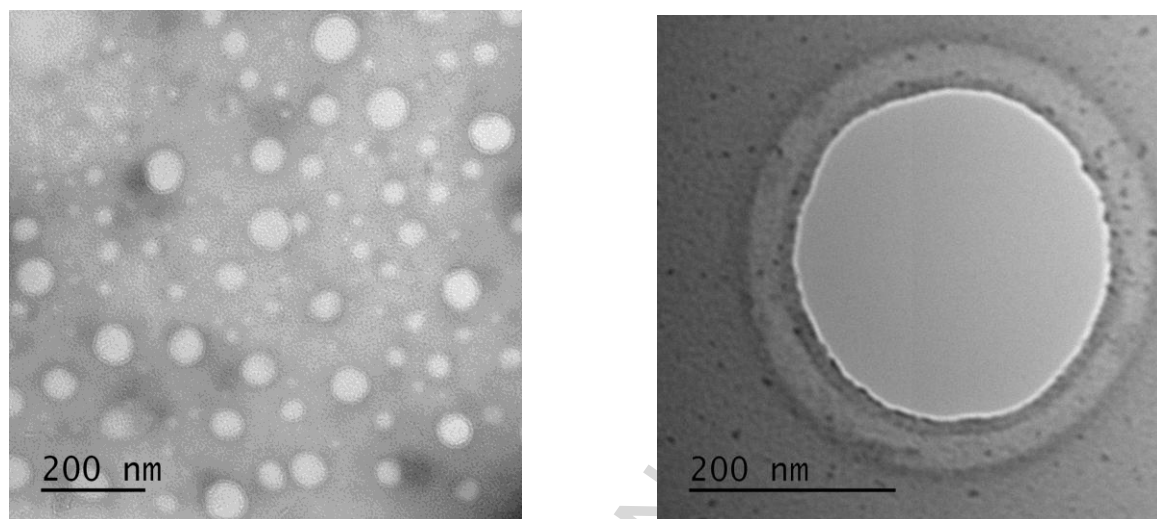


Figure 2. TEM image of pGlu₄₃-*b*-pPhe₂₉ (A) and pGlu₄₃-*b*-pPhe₄₉ (B) polymersomes.

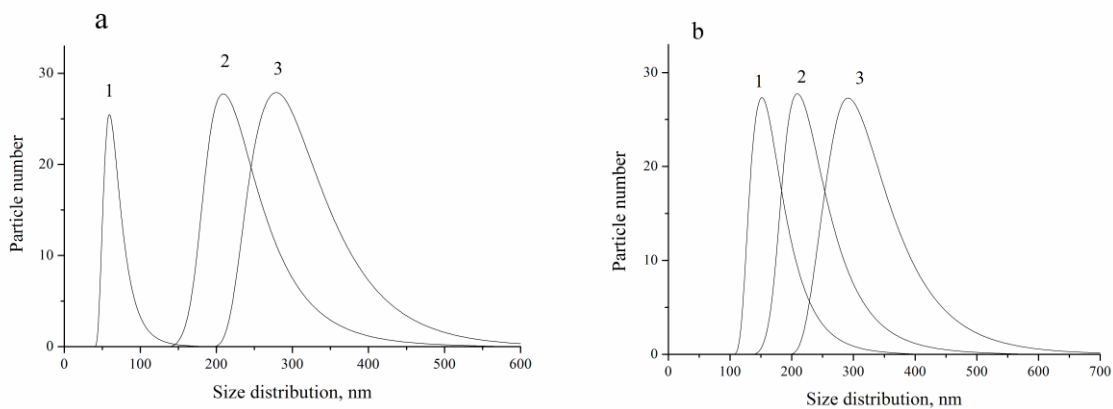


Figure 3. Dependence of (A) particle size distribution on hydrophobic part contribution at nanoparticle concentration 0.5 mg/mL 1 – TEMPO-pGlu₄₃-b-pPhe₁₂, 2 - TEMPO-pGlu₄₃-b-pPhe₂₉, 3 - TEMPO-pGlu₄₃-b-pPhe₄₉; and (B) particle size on the concentration of TEMPO-pGlu₄₃-b-Phe₂₉ 1 – 0.25 mg/mL, 2 – 0.5 mg/mL, 3 – 1.00 mg/mL.

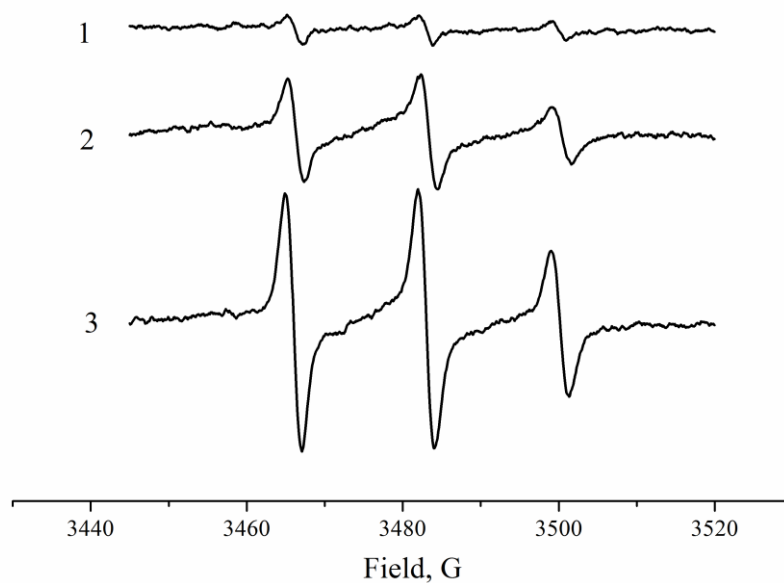


Figure 4. EPR spectra of 0.5 mg/mL suspensions of 1 – TEMPO-pGlu₄₃-*b*-pPhe₁₂, 2 - TEM-PO-pGlu₄₃-*b*-pPhe₂₉, 3 - TEMPO-pGlu₄₃-*b*-pPhe₄₉.

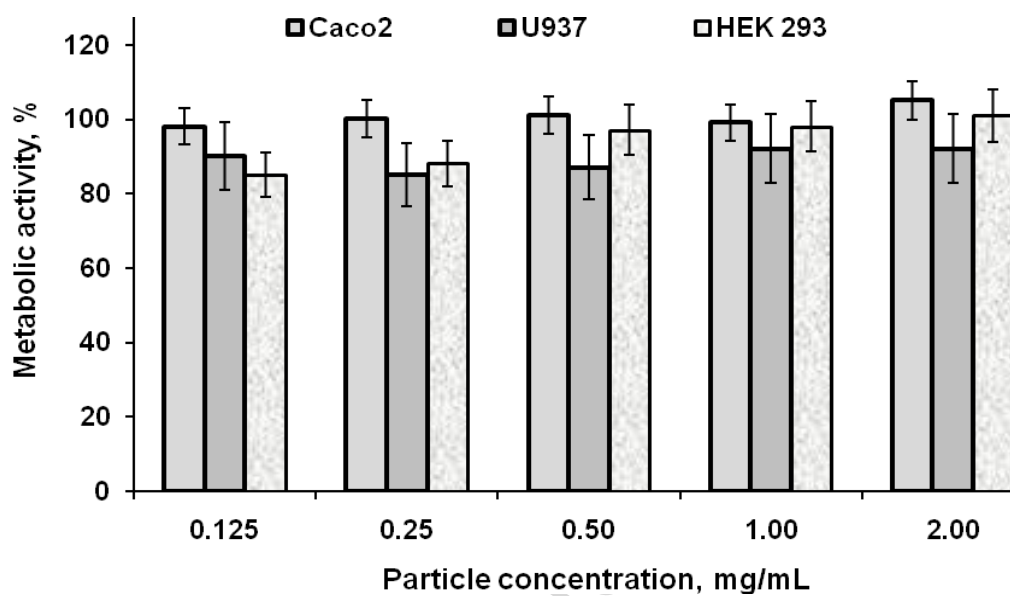


Figure 5. Viability of different cells incubated with TEMPO-pGlu₄₃-b-pPhe₂₉ polymersomes.

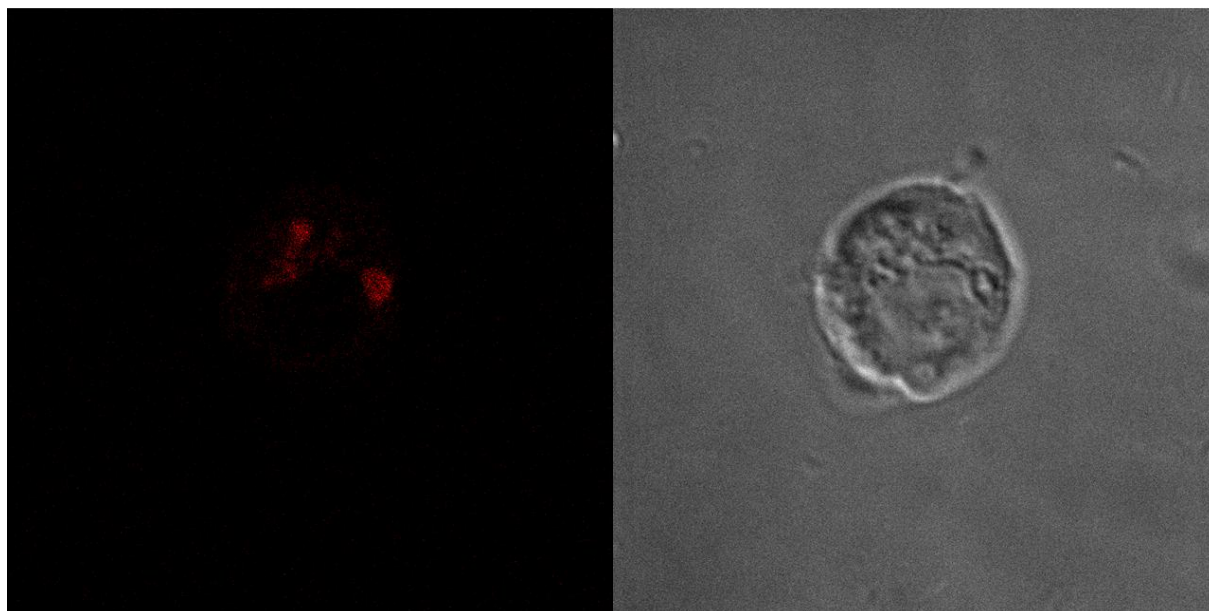


Figure 6. Confocal fluorescent (A) and bright-field images of U937 cell containing stained TEMPO-pGlu₄₃-*b*-pPhe₂₉ particles.

ACCEPTED MANUSCRIPT

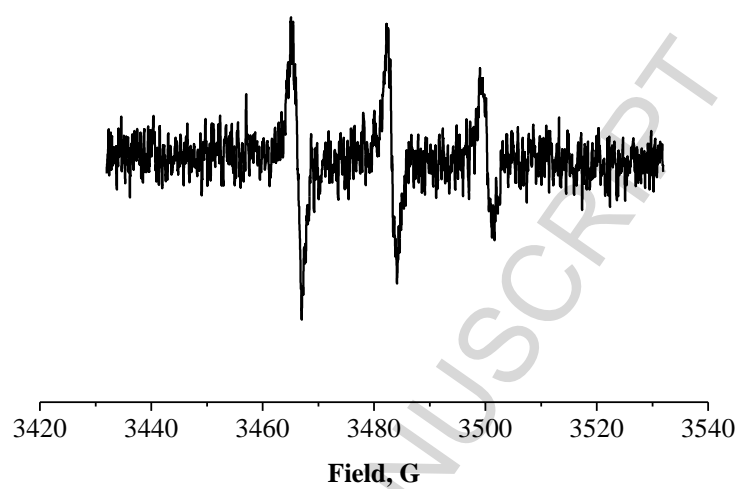


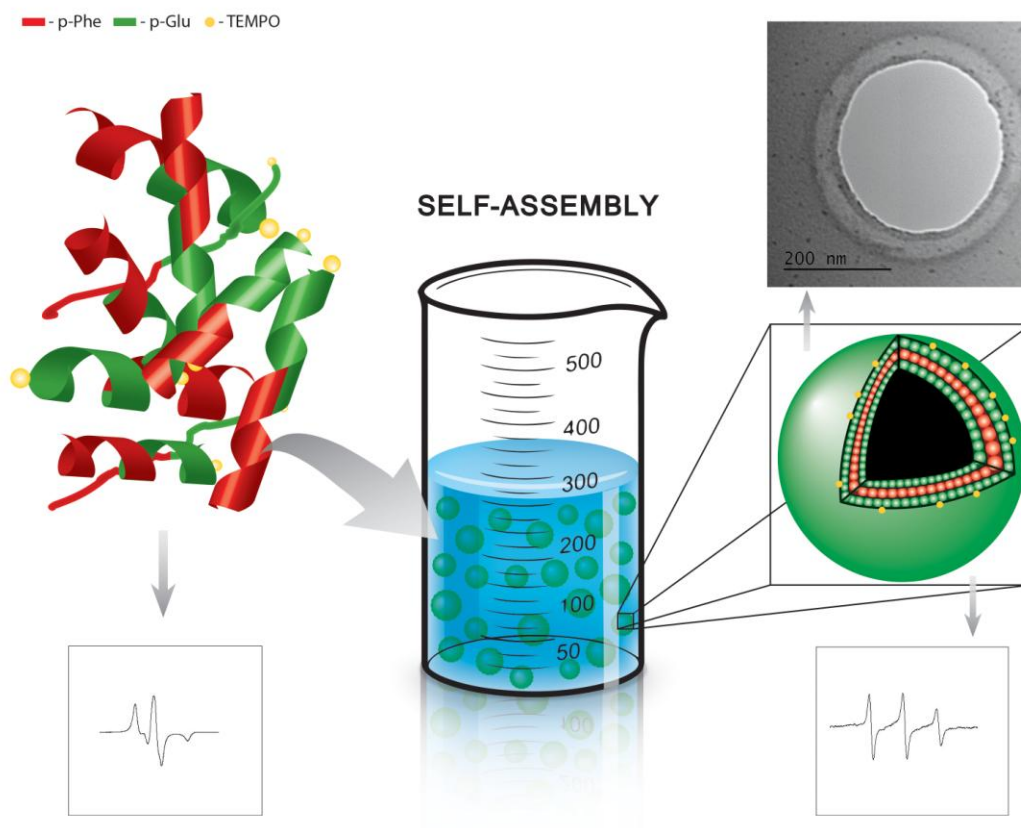
Figure 7. EPR spectrum of TEMPO-pGlu₄₃-b-pPhe₂₉ polymersomes after their penetration into U937 cells.

Table 1. Parameters of EPR spectra of the samples.

| Sample | $2A_{\parallel 1}$ G | $A_{\parallel 2}$ G | g_1 | g_2 | ϵ |
|---|-------------------------|------------------------|--------|--------|------------|
| APTES-p- γ - Glu(Bzl) | 44.2 | 65.4 | 2.0061 | 2.0029 | 0.338 |
| APTES-p- γ - Glu(Bzl)- <i>b</i> -pPhe | 35.1 | 64.4 | 2.0070 | 2.0068 | 0.269 |
| APTES-pGlu- <i>b</i> - pPhe | 35.6 | 68.1 | 2.0059 | 2.0024 | 0.097 |
| TEMPO-p- γ - Glu(Bzl) | 65.20 | - | 2.0060 | - | - |
| TEMPO-p- γ Glu(OBzl) ₄₃ - <i>b</i> - pPhe ₄₉ | 65.09 | - | 2.0061 | - | - |
| TEMPO-p- γ Glu ₄₃ - <i>b</i> -pPhe ₄₉ | 67.09 | - | 2.0060 | - | - |

Table 2. Parameters calculated from the nanoparticle suspensions EPR spectra

| Sample | a_N | T s | Rh, (Stokes-Einstein) m | C mole/L |
|---|-------------------------|-----------------------|------------------------------------|----------------------|
| TEMPO-pGlu ₄₃ - <i>b</i> -pPhe ₁₂ | 16.94 | 7.7×10^{-10} | 9.34×10^{-10} | 2.4×10^{-6} |
| TEMPO-pGlu ₄₃ - <i>b</i> -pPhe ₂₉ | 17.07 | 4.5×10^{-10} | 4.88×10^{-10} | 1.4×10^{-5} |
| TEMPO-pGlu ₄₃ - <i>b</i> -pPhe ₄₉ | 17.08 | 4.1×10^{-10} | 2.68×10^{-10} | 2.0×10^{-5} |



Graphical abstract

ACCEPTED